Cellular/Molecular

Localization of Diacylglycerol Lipase-α around Postsynaptic Spine Suggests Close Proximity between Production Site of an Endocannabinoid, 2-Arachidonoyl-glycerol, and Presynaptic Cannabinoid CB1 Receptor

Takayuki Yoshida,[1,2,3] Masahiro Fukaya,[1] Motokazu Uchigashima,[1] Eriko Miura,[1] Haruyuki Kamiya,[2] Masanobu Kano,[3] and Masahiko Watanabe[1]

Departments of [1]Anatomy or [2]Molecular Neuroanatomy, Hokkaido University School of Medicine, Sapporo 060-8638, Japan, and [3]Department of Cellular Neuroscience, Graduate School of Medical Science, Osaka University, Suita 565-0871, Japan

2-Arachidonoyl-glycerol (2-AG) is an endocannabinoid that is released from postsynaptic neurons, acts retrogradely on presynaptic cannabinoid receptor CB1, and induces short- and long-term suppression of transmitter release. To understand the mechanisms of the 2-AG-mediated retrograde modulation, we investigated subcellular localization of a major 2-AG biosynthetic enzyme, diacylglycerol lipase-α (DAGLα), by using immunofluorescence and immunoelectron microscopy in the mouse brain. In the cerebellum, DAGLα was predominantly expressed in Purkinje cells. DAGLα was detected on the dendritic surface and occasionally on the somatic surface, with a distal-to-proximal gradient from spiny branchlets toward somata. DAGLα was highly concentrated at the base of spine neck and also accumulated with much lower density on somatodendritic membrane around the spine neck. However, DAGLα was excluded from the main body of spine neck and head. In hippocampal pyramidal cells, DAGLα was also accumulated in spines. In contrast to the distribution in Purkinje cells, DAGLα was distributed in the spine head, neck, or both, whereas somatodendritic membrane was labeled very weakly. These results indicate that DAGLα is essentially targeted to postsynaptic spines in cerebellar and hippocampal neurons, but its fine distribution within and around spines is differently regulated between the two neurons. The preferential spine targeting should enable efficient 2-AG production on excitatory synaptic activity and its swift retrograde modulation onto nearby presynaptic terminals expressing CB1. Furthermore, different fine localization within and around spines suggests that the distance between postsynaptic 2-AG production site and presynaptic CB1 is differentially controlled depending on neuron types.

Key words: **endocannabinoid; 2-arachidonoyl-glycerol; 2-AG; diacylglycerol lipase; DAGL; CB1; immunohistochemistry; Purkinje cell; hippocampal pyramidal cell; mouse**

Introduction

Endogenous cannabinoids (endocannabinoids) are released from postsynaptic neurons and act retrogradely on presynaptic cannabinoid receptors, causing short- and long-term suppression of transmitter release. Endocannabinoid-mediated retrograde suppression (ERS) was found originally in the cerebellum (Kreitzer and Regehr, 2001a; Maejima et al., 2001) and hippocampus (Ohno-Shosaku et al., 2001; Wilson and Nicoll, 2001) and later in other brain regions (Alger, 2002; Wilson and Nicoll, 2002; Piomelli, 2003). ERS can be triggered by three distinct modes: membrane depolarization that elevates intracellular calcium concentration ($[Ca^{2+}]_i$) to a micromolar range (Brenowitz and Regehr, 2003), activation of the Gq-protein-coupled metabotropic receptor/phospholipase Cβ (PLCβ) pathway leading to the production of diacylglycerol (DAG) (Maejima et al., 2001; Kim et al., 2002; Ohno-Shosaku et al., 2003), and cooperative action of $[Ca^{2+}]_i$ elevation and Gq-protein-coupled receptor activation (Varma et al., 2001; Ohno-Shosaku et al., 2002; Hashimotodani et al., 2005; Maejima et al., 2005). Of these, the third mode appears physiologically most relevant, because ERS is induced by weak activation of Gq-protein-coupled receptors and physiological $[Ca^{2+}]_i$ increase to a submicromolar range, either of which is subthreshold for ERS by itself (Hashimotodani et al., 2005; Maejima et al., 2005).

Cannabinoid receptor CB1 is expressed predominantly in the nervous system, whereas CB2 is present in the immune system (Matsuda et al., 1990; Howlett et al., 2002). Immunohistochemical, biochemical, and electrophysiological studies using CB1 knock-out mice have provided evidence that CB1 is the major presynaptic cannabinoid receptor at inhibitory and excitatory synapses in various brain regions (Katona et al., 1999, 2001; Farquhar-Smith et al., 2000; Hajos et al., 2000, 2001; Wilson and

Received Jan. 6, 2006; revised March 18, 2006; accepted March 20, 2006.

This investigation was supported in part by a Grant-in-Aid for Scientific Research on Priority Areas and Special Coordination Funds for Promoting Science and Technology from the Ministry of Education, Culture, Sports, Science, and Technology, Japan.

Correspondence should be addressed to Masahiko Watanabe, Department of Anatomy, Hokkaido University School of Medicine, Sapporo 060-8638, Japan. E-mail: watamasa@med.hokudai.ac.jp.

DOI:10.1523/JNEUROSCI.0054-06.2006

 0270-6474/06/264740-12$15.00/0

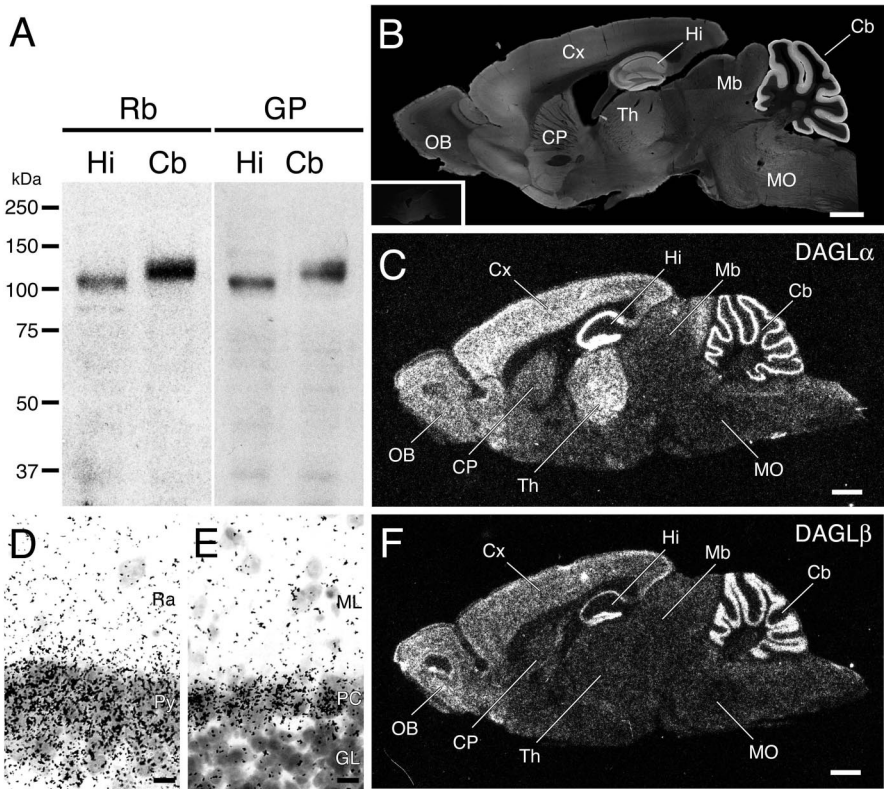

Figure 1. Specificity of DAGLα antibody and immunohistochemistry. ***A***, Immunoblot. Rabbit (Rb) and guinea pig (GP) antibodies to DAGLα recognize a 105 or 120 kDa protein band in the hippocampus (Hi) and cerebellum (Cb), respectively. The position of standard protein markers is indicated to the left (kDa). ***B***, Immunofluorescence for DAGLα in the adult mouse brain. Inset shows blank immunostaining in a control experiment using antibody preabsorbed with antigen. ***C–F***, *In situ* hybridization for DAGLα (***C–E***) and DAGLβ (***F***) mRNAs in the adult mouse brain. CP, Caudate–putamen; Cx, cerebral cortex; GL, granular layer; Mb, midbrain; ML, molecular layer; MO, medulla oblongata; OB, olfactory bulb; PC, Purkinje cell layer; Py, pyramidal cell layer; Ra, stratum radiatum; Th, thalamus. Scale bars: ***B***, ***C***, ***F***, 1 mm; ***D***, ***E***, 10 μm.

Nicoll, 2001; Yoshida et al., 2002; Bodor et al., 2005; Kofalvi et al., 2005; Kawamura et al., 2006). Intriguingly, CB1 is expressed in distinct interneuron subclasses in the hippocampus and also expressed in variable amounts at inhibitory and excitatory synapses in given neural regions (Katona et al., 1999; Hajos et al., 2000; Kawamura et al., 2006), suggesting its importance in information processing and integration (Freund, 2003).

2-Arachidonoyl-glycerol (2-AG) is one of the two major endocannabinoids (Devane et al., 1992; Mechoulam et al., 1995; Sugiura et al., 1995) and is synthesized on demand from DAG by *sn*-1-specific diacylglycerol lipase (DAGL) (Stella et al., 1997). Experiments with 2-AG synthesis inhibitors showed that 2-AG indeed mediates short- and long-term ERS (Melis et al., 2004; Safo and Regehr, 2005). Therefore, it is of great importance to clarify the site of DAGL expression to determine the site of 2-AG synthesis. Here we demonstrate that DAGLα, one of the two DAGLs cloned to date (Bisogno et al., 2003), is essentially targeted to postsynaptic spines. DAGLα is highly enriched at the base of spine neck but excluded from the main body of spines in cerebellar Purkinje cells, whereas DAGLα is distributed at the spine head, neck, or both in hippocampal pyramidal cells. The different fine localization in given neuron types suggests that specificity and efficiency of ERS depend not only on CB1 expression levels in presynaptic elements but also on the distance between postsynaptic 2-AG production site and presynaptic CB1.

Materials and Methods

Animal and section preparation. C57BL mice at the adult stage (2–4 months of age) and postnatal day 10 (P10) were used in the present study. Under deep pentobarbital anesthesia (100 mg/kg body weight, i.p.), brains were freshly removed from the skull and frozen in powdered dry ice for *in situ* hybridization. Frozen sections were prepared on a cryostat (20 μm in thickness; CM1900; Leica, Nussloch, Germany) and mounted on silane-coated glass slides (Muto-Glass, Tokyo, Japan). For immunohistochemistry, anesthetized mice were fixed transcardially with 4% paraformaldehyde in 0.1 M sodium phosphate buffer (PB), pH 7.2, for light microscopy or 4% paraformaldehyde/0.1% glutaraldehyde in PB for electron microscopy, and microslicer sections (50 μm) were prepared (VT1000S; Leica).

In situ *hybridization.* Fresh frozen sections were treated at room temperature with the following incubations: fixation with 4% paraformaldehyde in PB for 10 min, 2 mg/ml glycine–PBS, pH 7.2, for 10 min, acetylation with 0.25% acetic anhydride in 0.1 M triethanolamine-HCl, pH 8.0, for 10 min, and prehybridization for 1 h in a buffer containing 50% formamide, 50 mM Tris-HCl, pH 7.5, 0.02% Ficoll, 0.02% polyvinylpyrrolidone, 0.02% bovine serum albumin (BSA), 0.6 M NaCl, 0.25% SDS, 200 μg/ml tRNA, 1 mM EDTA, and 10% dextran sulfate. Hybridization was performed at 42°C for 12 h in the prehybridization buffer supplemented with 10,000 cpm/μl [^{33}P]dATP-labeled antisense oligonucleotide probes. Probes were synthesized against nucleotide residues 3016–3060 of the mouse DAGLα cDNA (GenBank accession number NM198114) and 1996–2040 of the mouse DAGLβ cDNA (GenBank accession number BC016105) and labeled using terminal deoxyribonucleotidyl transferase (Invitrogen, Carlsbad, CA). Slides were washed twice at 55°C for 40 min in 0.1× SSC containing 0.1% sarcosyl. Sections were exposed to BioMax film (Eastman Kodak, Rochester, NY) for 4 weeks.

Antibody. We used affinity-purified primary antibodies raised against the following molecules (species immunized): mouse DAGLα (rabbit and guinea pig, see below); mouse protein kinase Cγ (PKCγ) (rabbit and guinea pig; see below); mouse calbindin [goat (Miura et al., 2006)]; mouse microtubule-associated protein-2 (MAP2) [goat (Miura et al., 2006)]; mouse parvalbumin [guinea pig (Nakamura et al., 2004)]; mouse PLCβ4 [rabbit and guinea pig (Nakamura et al., 2004)]; mouse 3-phosphoglycerate dehydrogenase (3PGDH) [guinea pig (Yamasaki et al., 2001)]; rat vesicular glutamate transporter 1 (VGluT1) and 2 (VGluT2) [guinea pig (Miyazaki et al., 2003)]; mouse vesicular γ-aminobutylic acid transporter (VGAT) [guinea pig (Miyazaki et al., 2003)]; mouse cannabinoid CB1 receptor [guinea pig (Fukudome et al., 2004)]; and mouse type 1α metabotropic glutamate receptor (mGluR1α) [rabbit (Tanaka et al., 2000)].

For production of antibodies, cDNA fragments, which are preceded with a *Bam*HI site and encode C-terminal 42 amino acids of DAGLα (1003–1044 amino acid residues; GenBank accession number NM198114) or C-terminal 14 amino acids of PKCγ (684–697; GenBank accession number L28035), were obtained by PCR or by annealing of sense and antisense oligonucleotides, respectively. After the thymidine/adenosine (TA) cloning using a pGEM-T Easy Vector System I kit (Promega, Madison, WI), cDNA fragments was sequenced and excised by *Bam*HI and *Eco*RI. These fragments were subcloned into *Bam*HI/*Eco*RI site of pGEX4T-2 plasmid (Amersham Biosciences, Piscataway, NJ) for

expression of glutathione *S*-transferase (GST) fusion proteins. GST fusion proteins were purified using glutathione-Sepharose 4B (Amersham Biosciences), according to the instructions of the manufacturer, and used for immunization to New Zealand White rabbits and Hartley guinea pigs. Antigens were emulsified with Freund's complete or incomplete adjuvant (Difco, Detroit, MI) and injected subcutaneously at intervals of 2 weeks. After the sixth injection, Ig specific to antigens were affinity purified using GST-free peptides coupled to cyanogen bromide-activated Sepharose 4B (Amersham Biosciences). GST-free peptides were prepared by in-column thrombin digestion of GST fusion proteins bound to glutathione-Sepharose 4B media.

Western blotting. The hippocampus and cerebellum were homogenized using a Potter homogenizer with 15 strokes at 1000 rpm in 10 vol of ice-cold homogenizer buffer containing 0.32 M sucrose, 1 mM EDTA, 1 mM EGTA, 10 mM Tris-HCl, pH 7.2, and 0.4 mM phenylmethylsulfonyl fluoride. The protein concentration was determined by the Lowry's method. The homogenates were denatured by 50 mM (±)-dithiothreitol at 65°C for 15 min. Proteins (15 μg/lane) were separated by SDS-PAGE and electroblotted onto nitrocellulose membranes (BioTraceNT; Pall Gelman Laboratory, Ann Arbor, MI). After blocking with 5% skimmed milk for 30 min, membranes were incubated for 2 h with rabbit or guinea pig DAGLα antibody (1 μg/ml). Tris-buffered saline, pH 7.5, containing 0.1% Tween 20 was used for diluent and washing buffer. Immunoreaction was visualized with the ECL chemiluminescence detection system (Amersham Biosciences).

Immunohistochemistry. All immunohistochemical incubations were done at room temperature in a free-floating state. For immunofluorescence, cerebellar sections were incubated with 10% normal donkey serum for 30 min, a mixture of primary antibodies overnight (1 μg/ml), and a mixture of Alexa Fluor-488-, indocarbocyanine (Cy3), and indodicarbocyanine (Cy5)-labeled species-specific secondary antibodies for 2 h at a dilution of 1:200 (Invitrogen; Jackson ImmunoResearch, West Grove, PA). For hippocampal sections, immunofluorescence was performed by two-step method, as follows. First, sections were incubated with 10% normal donkey serum for 30 min, rabbit DAGLα antibody (0.5 μg/ml) overnight, biotinylated secondary antibody for 2 h, and streptavidin–peroxidase complex for 30 min using a Histofine SAB-PO(R) kit (Nichirei, Tokyo, Japan), followed by visualization using a tyramide signal amplification kit [TSA-DIRECT (Red); NEN, Boston, MA]. After blocking with 10% normal rabbit serum, conventional immunofluorescence was then used as above. PBS containing 0.1% Tween 20 was used for diluent of antibodies and washing buffer. Images were taken with a fluorescence microscope (AX-70; Olympus Optical, Tokyo, Japan) equipped with a digital camera (DP70; Olympus Optical) or with a confocal laser scanning microscope (FV1000; Olympus Optical).

For immunoperoxidase electron microscopy, microslicer sections were incubated successively with 10% normal donkey serum, rabbit DAGLα antibody (0.5–2 μg/ml), biotinylated secondary antibody, and streptavidin–peroxidase complex as above. Immunoreaction was visualized with 3,3′-diaminobenzidine. For preembedding immunogold electron microscopy, microslicer sections were dipped in 5% BSA/0.02% saponin/PBS for 30 min, and incubated overnight with rabbit DAGLα (0.5–2 μg/ml), guinea pig CB1 (1 μg/ml), or rabbit PKCγ (1 μg/ml) antibody diluted with 1% BSA/0.004% saponin/PBS and then with anti-rabbit IgG linked to 1.4 nm gold particles (Nanogold; Nanoprobes, Stony Brook, NY) for 2 h. Immunogolds were intensified with a silver enhancement kit (HQ silver; Nanoprobes). Sections labeled by immunoperoxidase and silver-enhanced immunogold were treated with 2% osmium tetroxide for 30 min, stained in block with 2% uranyl acetate for 30 min, dehydrated, and embedded in Epon 812.

For postembedding immunogold electron microscopy, microslicer sections were cryoprotected with 30% sucrose/PB and frozen rapidly with liquid propane in an EM CPC unit (Leica). Frozen sections were immersed in 0.5% uranyl acetate in methanol at −90°C in an AFS freeze-substitution unit (Leica), infiltrated at −45°C with Lowicryl HM-20 resin (Lowi, Waldkraiburg, Germany), and polymerized with UV light. After etching with saturated sodium-ethanolate solution for 3 s, ultrathin sections on nickel grids were treated successively with 2% human serum albumin (Wako, Osaka, Japan)/0.1% Tween 20 in Tris-buffered saline, pH 7.5 (HTBST) for 30 min, rabbit DAGLα antibody (15 μg/ml) in

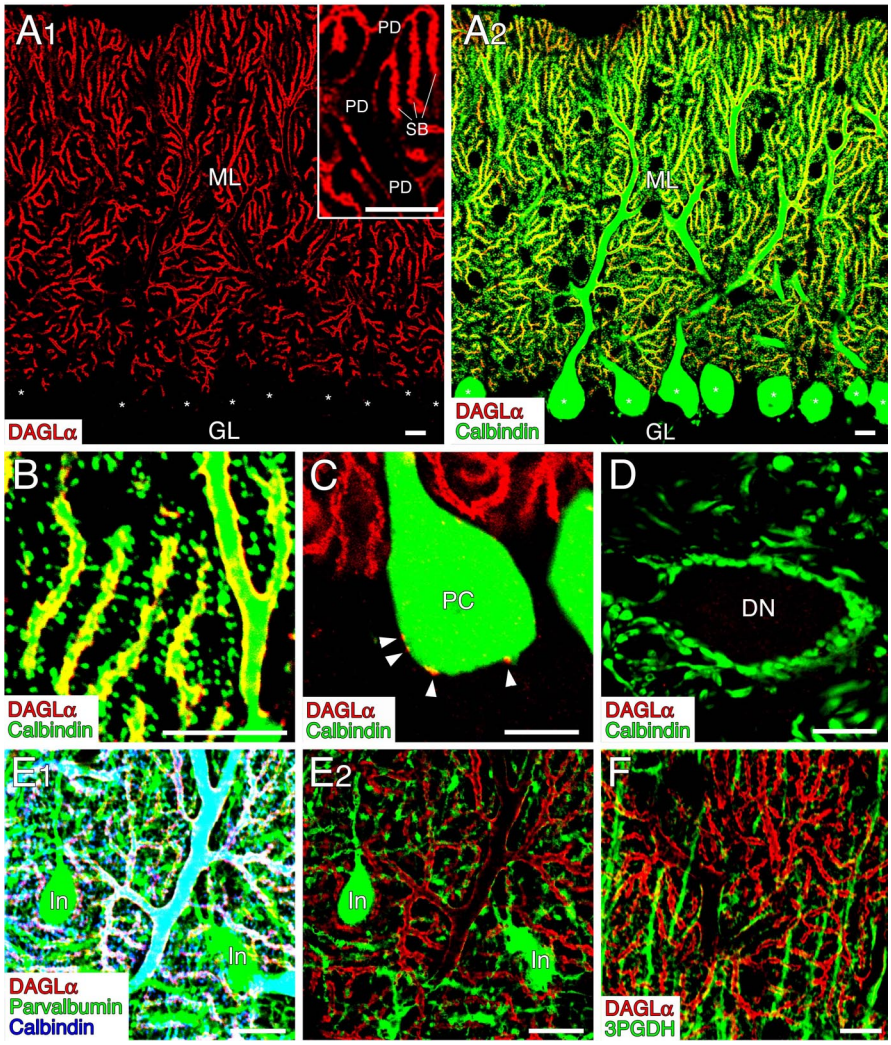

Figure 2. Immunofluorescence showing Purkinje cell-specific and somatodendritic distribution of DAGLα in the cerebellum. ***A–D***, Double immunofluorescence for DAGLα (red) and calbindin (green). ***E***, Triple immunofluorescence for DAGLα (red), parvalbumin (green), and calbindin (blue). ***F***, Double immunofluorescence for DAGLα (red) and 3PGDH (green). ***A***, Predominant distribution of DAGLα in Purkinje cell dendrites in the molecular layer (ML). Inset in ***A1*** is an enlarged view showing stronger immunolabeling in spiny branchlets (SB) than in thick proximal dendrites (PD). Asterisks indicate Purkinje cell somata. ***B***, Lack of DAGLα in dendritic spines. ***C***, Occasional labeling of DAGLα in Purkinje cell soma (PC, arrowheads). ***D***, Lack of DAGLα in Purkinje cell terminals on neurons in the deep cerebellar nuclei (DN). ***E***, Lack of DAGLα in molecular layer interneurons (In). ***E2*** is an image in which the light blue color is subtracted from ***E1***. ***F***, Lack of DAGLα in Bergmann glia. GL, Granular layer. Scale bars, 10 μm.

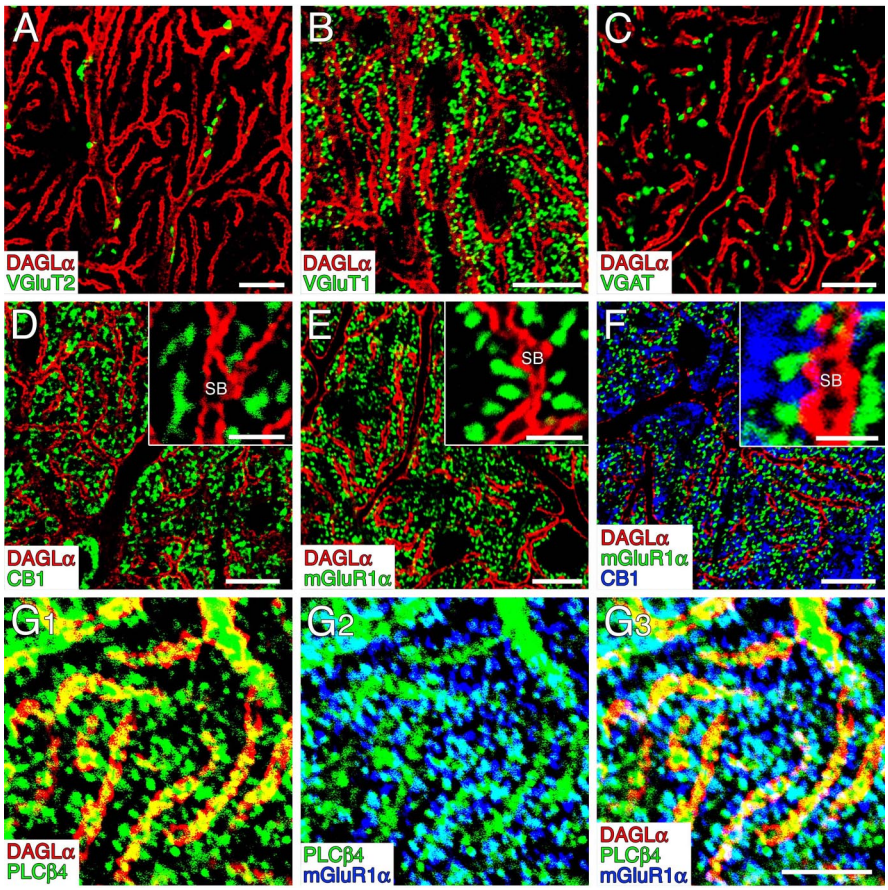

Figure 3. Immunofluorescence showing anatomical relationship of DAGLα distribution with presynaptic and postsynaptic molecules. In all images, DAGLα is in red. ***A–C***, Lack of DAGLα in VGluT2-labeled climbing fiber terminals (***A***), VGluT1-labeled parallel fiber terminals (***B***), and VGAT-labeled inhibitory interneuron terminals (***C***). ***D–F***, DAGLα on spiny branchlets (SB) is distributed closely to but separated from CB1 (green in ***D***; blue in ***F***) or mGluR1α (green in ***E***, ***F***). ***G***, Triple immunostaining for DAGLα, PLCβ4 (green), and mGluR1α (blue). Note overlap of PLCβ4 with DAGLα in dendritic shafts and with mGluR1α in dendritic spines. Scale bars: ***A–F***, 10 μm; ***G***, 5 μm; insets in ***D–F***, 2 μm.

HTBST overnight, and colloidal gold (10 nm)-conjugated anti-rabbit IgG (1:100; British Bio Cell International, Cardiff, UK) in HTBST for 2 h. Finally, grids were stained with 2% uranyl acetate for 20 min and with mixed lead solution for 30 s. Photographs were taken with an H-7100 electron microscope (Hitachi, Tokyo, Japan).

For quantitative analysis, silver-enhanced immunogold particles for DAGLα on somatodendritic and spine membranes or for CB1 on parallel fibers were counted on electron micrographs. Furthermore, tangential and perpendicular distributions of DAGLα in spines were examined from 57 spines of parallel fiber–Purkinje cell synapses (postembedding immunogold) and 49 spines of CA1 pyramidal cell synapses (preembedding immunogold) and analyzed using IPLab software (Nippon Roper, Tokyo, Japan).

Results

Specificity of DAGLα antibody and immunohistochemistry

We produced polyclonal rabbit and guinea pig antibodies against C-terminal sequence of mouse DAGLα. After affinity purification, both antibodies selectively recognized protein bands at 105 kDa in the hippocampus and at 120 kDa in the cerebellum (Fig. 1*A*). The molecular mass of the cerebellar band was almost similar to that reported previously (Bisogno et al., 2003). By immunofluorescence with parasagittal brain sections, the highest immunoreactivity was detected in the cerebellar cortex and hippocampus (Fig. 1*B*). Moderate levels were detected in the cerebral cortex, olfactory bulb, caudate–putamen, and thalamus. The spatial patterns of immunostaining were essentially the same with use of rabbit and guinea pig antibodies. Preabsorption of antibodies with antigen protein abolished the immunostaining (Fig. 1*B*, inset).

This immunostaining was compared with the distribution of DAGLα and DAGLβ mRNAs. DAGLα mRNA was expressed at the highest level in the hippocampus and cerebellar cortex, in which autoradiographic silver grains were observed on hippocampal pyramidal cells, dentate granule cells, and cerebellar Purkinje cells but not on hippocampal nonpyramidal cells or cerebellar granule cells (Fig. 1*C–E*). Moderate expression of DAGLα mRNA was noted in the cerebral cortex, olfactory bulb, and thalamus. DAGLβ mRNA also showed wide expression in the brain with particular abundance in the cerebral and cerebellar cortices, olfactory bulb, and dentate gyrus (Fig. 1*F*). However, its distribution differed from that of DAGLα mRNA in that DAGLβ mRNA was expressed at the highest level in the cerebellar granular layer and relatively low in the hippocampal pyramidal cell layer and thalamus. These signals were abolished almost completely by addition of an excess amount of cold probes in the hybridization mixture (data not shown). Because Purkinje cells were predominantly immunolabeled in the cerebellum (see below), the pattern of immunostaining is thus similar to DAGLα mRNA expression, suggesting that antibodies produced in the present study are specific to DAGLα.

We applied these antibodies to examine cellular expression and subcellular distribution in the cerebellum (see Figs. 2–7) and hippocampus (see Figs. 8, 9). In multiple labeling, DAGLα is in red and others are in green or blue throughout the present study.

Somatodendritic surface expression of DAGLα in Purkinje cell

In the cerebellum, DAGLα staining was virtually confined to the molecular layer, in which a tubular or cylindrical pattern of immunostaining was evident (Fig. 2*A1*). DAGLα expression in Purkinje cells was examined by double immunofluorescence with calbindin (Fig. 2*A–D*). DAGLα staining was most intense and continuous on spiny branchlets (or distal dendrites), but spines emitting from spiny branchlets appeared to lack the labeling (Fig. 2*A1*, inset, *B*). The intensity became lowered and intermittent on proximal dendrites (Fig. 2*A1*, inset). In the soma of Purkinje cells, weak and spotty labeling was occasionally detected on the somatic surface (Fig. 2*C*). In contrast, DAGLα labeling was not detected in axon terminals of Purkinje cells, which form synapses on neurons in the deep cerebellar nucleus (Fig. 2*D*). Expression of DAGLα in molecular layer interneurons was examined by triple immunofluorescence for calbindin (blue), parvalbumin (green), and DAGLα (Fig. 2*E1*). It is known that Purkinje

cells express both calbindin and parvalbumin (light blue), whereas molecular layer interneurons express parvalbumin only (green). By subtracting the light blue color (representing Purkinje cell dendrites) from Figure 2*E1*, dendrites, cell bodies, and axons of interneurons were selectively visualized as green elements, but they lacked DAGLα (Fig. 2*E2*). Possible expression of DAGLα in Bergmann glia was examined by double immunofluorescence for DAGLα and 3PGDH, a serine biosynthetic enzyme expressed in Bergmann glia but not in Purkinje cells or other neurons (Yamasaki et al., 2001). 3PGDH-positive Bergmann fibers were devoid of DAGLα immunofluorescence (Fig. 2*F*). These results demonstrate that, in the cerebellum, DAGLα is predominantly expressed in Purkinje cells and localized to somatodendritic elements, particularly at high levels in spiny branchlets.

Close apposition of DAGLα to other endocannabinoid signaling molecules

Endocannabinoids are effectively synthesized in Purkinje cells by conjunctive synaptic activation of ionotropic AMPA receptor and mGluR1 (Maejima et al., 2001, 2005; Brown et al., 2003; Brenowitz and Regehr, 2005). Synaptic distribution of DAGLα was examined by multiple immunofluorescence for presynaptic markers and postsynaptic signaling molecules (Fig. 3). DAGLα was hardly detected in VGluT2-labeled climbing fiber terminals, VGluT1-labeled parallel fiber terminals, or VGAT-labeled interneuron terminals (Fig. 3*A–C*). Nonoverlapping pattern with presynaptic markers was also observed by double immunofluorescence for cannabinoid receptor CB1 (Fig. 3*D*), which is expressed in these afferents (Kawamura et al., 2006). Such nonoverlapping pattern was also seen for mGluR1α (Fig. 3*E*), which is concentrated on dendritic spines, particularly at the perisynaptic annulus surrounding the edge of synaptic junction (Baude et al., 1993; Nusser et al., 1994). Consequently, when triple immunofluorescence was performed for DAGLα, mGluR1α, and CB1, the three immunofluorescent signals were distributed in a mutually exclusive manner but closely apposed to one another (Fig. 3*F*). PLCβ4 is a major PLCβ subtype in Purkinje cells of the rostral cerebellum (Kano et al., 1998; Watanabe et al., 1998b) and was distributed in both spines and dendritic shafts (Nakamura et al., 2004). Immunofluorescence signals for PLCβ4 overlapped with those for mGluR1α in spines and with those for DAGLα in dendritic shafts (Fig. 3*G*). Therefore, DAGLα is localized close to CB1-carrying presynaptic elements and mGluR1α/PLCβ4-carrying postsynaptic spines but apart from both of them.

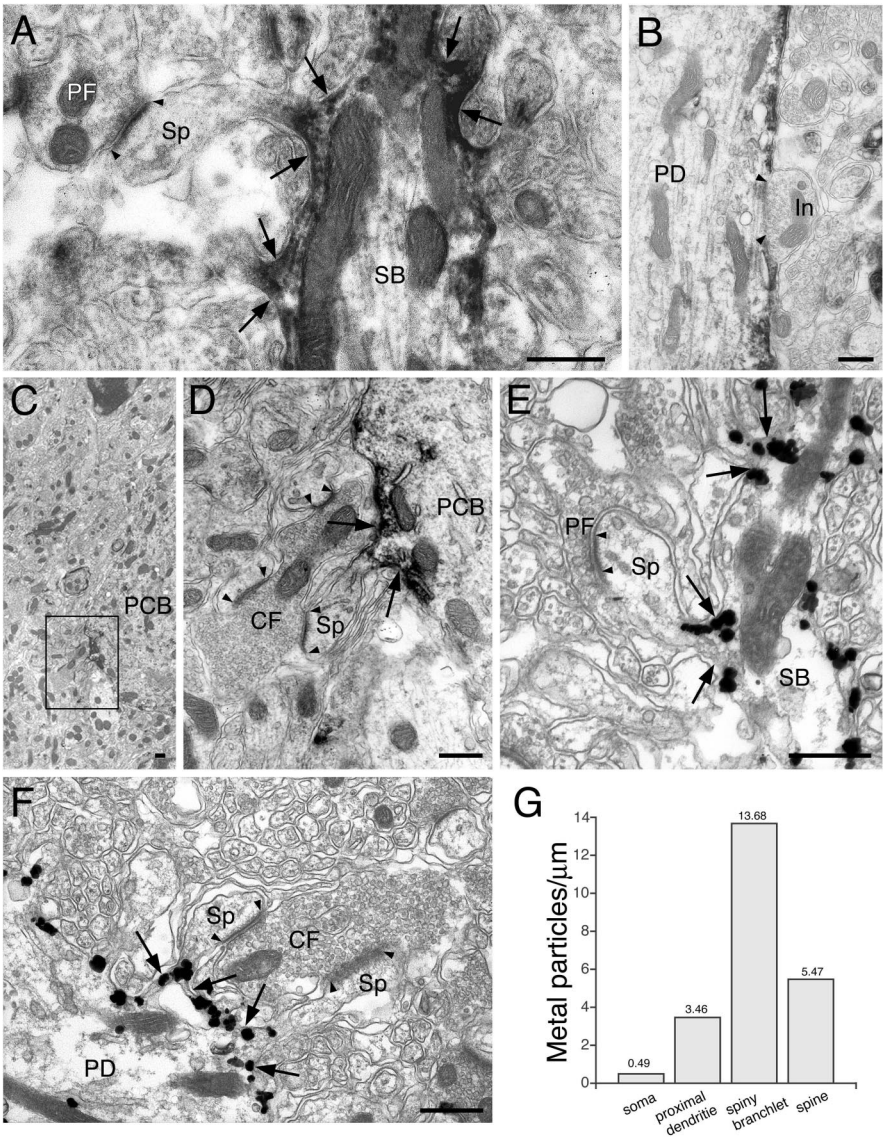

Figure 4. Preembedding immunoelectron microscopy showing selective somatodendritic surface expression of DAGLα in Purkinje cells. ***A–D***, Immunoperoxidase. ***E–G***, Silver-enhanced immunogold. ***A***, Spiny branchlet (SB). Note strong labeling on the surface of spiny branchlets but not in most portions of spines (Sp) contacting to parallel fiber terminals (PF). ***B***, Proximal dendrite (PD). Note the lack of DAGLα at synaptic junction with inhibitory terminals (In). ***C***, ***D***, Purkinje cell body (PCB). DAGLα labeling is seen at the base of somatic spine contacting with a climbing fiber terminal (CF) and also on the somatic cell membrane around the spine. ***D*** is an enlarged view of the boxed region in ***C***. ***E***, Spiny branchlet (SB). Note the dense immunogold labeling on spiny branchlets but not on most portions of spine contacting with a parallel fiber terminal (PF). ***F***, Proximal dendrite (PD). Immunogold labeling on proximal dendrites but not on most portions of spines contacting with a climbing fiber terminal (CF). ***G***, Histograms showing the density of immunogold labeling for DAGLα on each domain of Purkinje cells. The total length of measured cell membranes is 48.5 μm in the soma, 103.3 μm in proximal dendrites, 76.3 μm in spiny branchlets, and 39.9 μm in spines. Arrows and arrowheads indicate the border between spines and dendrites (or soma) or the edge of postsynaptic density, respectively. Scale bars, 0.5 μm.

Enriched localization of DAGLα at the base of spine neck and its adjacent somatodendritic membrane in Purkinje cell

Ultrastructural localization of DAGLα in Purkinje cells was investigated by immunoelectron microscopy (see Figs. 4, 5). By using the immunoperoxidase method, spiny branchlets were most strongly labeled (Fig. 4*A*), whereas proximal dendrites (Fig. 4*B*) and somata (Fig. 4*C*,*D*) were labeled at low to moderate levels. Even with a diffusible peroxidase substrate (i.e., diaminobenzidine), immunoreaction products were often concentrated in the cytoplasm just beneath the somatodendritic cell mem-

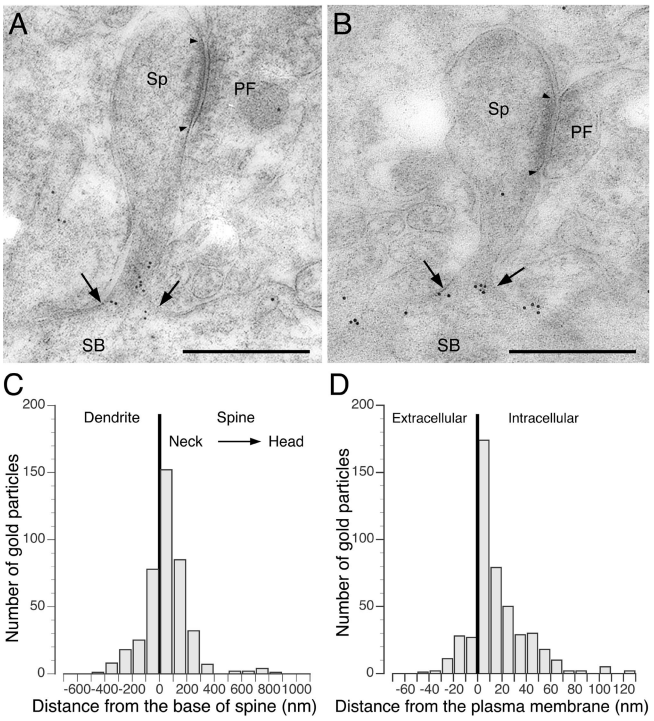

Figure 5. Postembedding immunogold for DAGLα in dendritic spines of Purkinje cells. ***A***, ***B***, Two longitudinally sectioned parallel fiber synapses contacting to spines (Sp) emitting from spiny branchlets (SB). Note the prominent accumulation of immunogold labeling at the base of the spine neck. Also note the lack of immunogold labeling on most other parts of spines, including the spine head. PF, Parallel fiber. ***C***, Histograms showing the distribution of gold particles within and around spines. The distance from the dendrite–spine border (0 nm in ***C***; arrows in ***A***, ***B***) is plotted in the abscissa. The ordinate indicates the number of gold particles in each 100 nm bin, being summed up from 57 spines analyzed ($n = 415$ immunogold particles). ***D***, Histograms showing the perpendicular distribution of DAGLα. The number of gold particles is plotted as a function of the distance from the midpoint of the plasma membrane to the center of gold particles ($n = 471$ immunogold particles). Arrowheads indicate the edge of postsynaptic density. Scale bars, 0.5 μm.

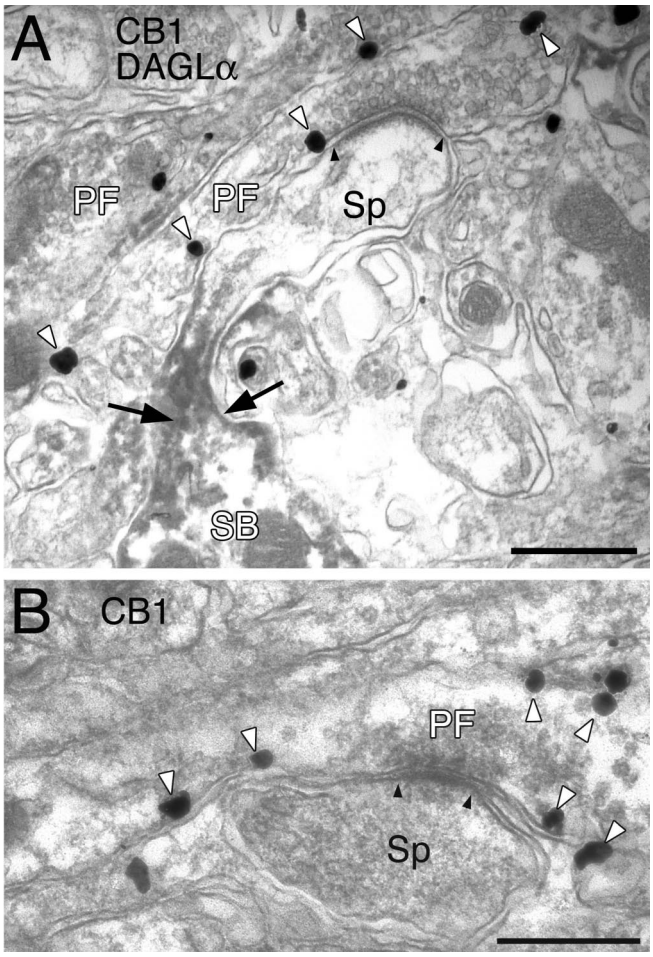

Figure 6. Localization of CB1 at parallel fiber–Purkinje cell synapses by silver-enhanced immunogold. ***A***, Double-immunoelectron microscopy by immunoperoxidase for DAGLα and by silver-enhanced immunogold for CB1 (open arrowheads). Arrows indicate the dendrite–spine border. ***B***, Distribution of CB1 (open arrowheads) in a longitudinally sectioned parallel fiber (PF) synapse. Note the higher labeling density on the axolemma-facing spine (Sp) than that of the opposite-facing side. SB, Spiny branchlet. Scale bars, 0.5 μm.

brane. Strong immunoreaction was observed in the neck of spines forming asymmetrical synapses with parallel fiber terminals (Fig. 4*A*), which were relatively small in size and contained a small number of synaptic vesicles accumulating near the synaptic junction. No immunoreaction was seen in the spine head (Fig. 4*A*) or at symmetrical synapses formed onto dendritic shaft (Fig. 4*B*). In perikarya, immunoperoxidase labeling was considerably rare but occasionally encountered (Fig. 4*C*). When carefully pursuing the labeled regions on serial sections, we found spines protruding from immunolabeled somatic membrane (Fig. 4*D*). Interestingly, somatic spines formed asymmetrical synapses with climbing fiber terminals, which were large in size and contained a large number of synaptic vesicles and dark cytoplasm. In such somatic spines, DAGLα labeling was also restricted to the neck region and its adjacent somatic membrane (Fig. 4*D*).

By using the preembedding silver-enhanced immunogold method, the cytoplasmic side of somatodendritic membrane was labeled. In spiny branchlets, metal particles representing DAGLα were associated with the cell membrane at the base of spine neck, whereas other regions of spines, including the head region, were little labeled (Fig. 4*E*). In proximal dendrites, DAGLα was distributed along the cell membrane but was excluded from the postsynaptic site of symmetrical synapses (data not shown). Spines emanating from proximal dendrites were much lower in density than those from spiny branchlets and were identified on serial sections to form synapses with climbing fiber terminals (Fig. 4*F*). Also in such spines, DAGLα was detected at the base of spine neck and its adjacent dendritic membrane. Using randomly taken electron micrographs, the number of metal particles per 1 μm of the cell membrane was measured for the soma, proximal dendrite, spiny branchlet, and spine. The highest density was shown in spiny branchlets, and the density was declined sharply toward the soma (Fig. 4*G*). Most particles that fell on the spine membrane were attributable to labeling in the neck portion.

Postsynaptic molecules, particularly those condensed at postsynaptic membrane or postsynaptic density, are often resistant to preembedding immunohistochemical detection because of limited antibody accessibility (Fritschy et al., 1998; Watanabe et al., 1998a; Fukaya and Watanabe, 2000). This can be overcome by the postembedding immunogold method (Baude et al., 1995; Ottersen and Landsend, 1997). We confirmed the lack of DAGLα labeling at synaptic junction by the postembedding immunogold method (Fig. 5*A*,*B*). Furthermore, this method disclosed that DAGLα was highly accumulated at the base of spine neck or the dendrite–spine border. This observation was quantitatively evaluated by counting the number of gold particles as a function of distance from the dendrite–spine border (Fig. 5*C*). The peak distribution was found at the 0–100 nm bin in the spine side, and

labeling was steeply decreased toward both the spine head and dendritic shaft ($n = 57$ spines). Then, we examined perpendicular distribution of DAGLα by measuring the distance from the midpoint of plasma membrane to the center of gold particles. The peak distribution was found at the 0–10 nm bin toward the intracellular side of the plasma membrane (Fig. 5*D*). Moreover, 82.3% of the total immunogold particles were located within 35 nm from the midpoint of the cell membrane, suggesting preferential cell membrane-associated distribution of DAGLα with the C-terminal epitope intracellularly. These results demonstrate that DAGLα is distributed on the somatodendritic cell membrane, particularly at high levels in the base of the spine neck. In contrast, DAGLα is selectively excluded from the spine head, on which excitatory afferents form asymmetrical synapses.

Because 2-AG synthesized by DAGLα presumably diffuses in the extracellular space and binds to CB1, it is important to clarify how CB1 is distributed on axons and terminals in relation to the 2-AG production site. Recently, we have shown that CB1 is highly accumulated on perisynaptic portion of parallel fibers (<500 nm from the edge of synaptic junction) (Kawamura et al., 2006). In the present study, we analyzed parallel fiber synapses sectioned longitudinally to compare the distribution of CB1 on parallel fibers between synaptic and opposite sides. We found that CB1 labeling was preferentially detected on the axolemma facing Purkinje cell spines (Fig. 6). There was almost twice the number of metal particles in the synaptic side of axolemma (69.2%) compared with the opposite side (30.8%; $n = 65$ total metal particles obtained from 17 parallel fiber synapses).

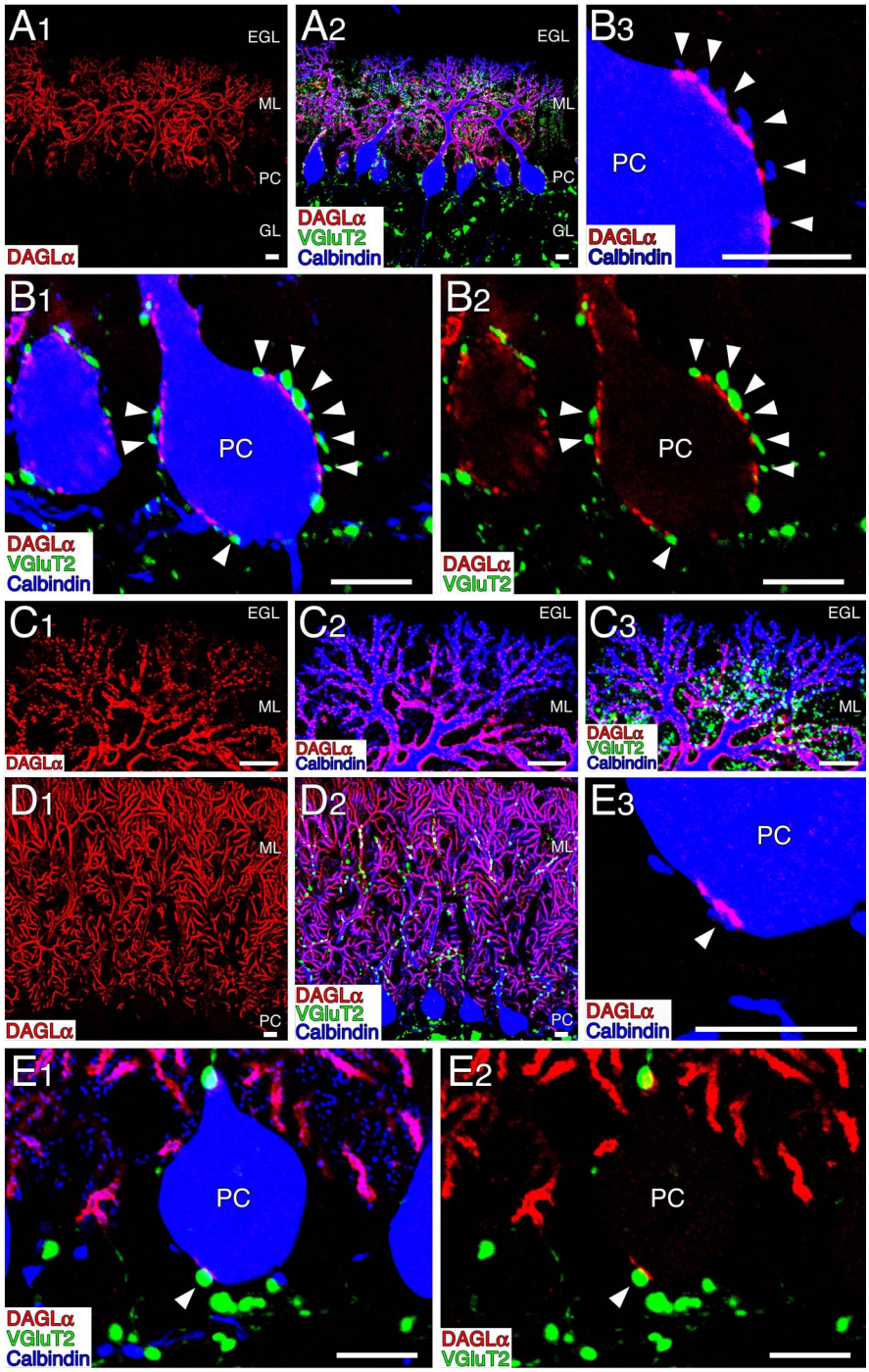

Figure 7. Spine- or synapse-associated expression of DAGLα in Purkinje cells at P10 (***A–C***) and adult (***D***, ***E***). Triple labeling for DAGLα (red), VGluT2 (green), and calbindin (blue). Portions of ***A*** and ***D*** are enlarged in ***B*** and ***C*** or in ***E***, respectively. Note that DAGLα is localized just beneath calbindin-stained somatic spines (arrowheads) and VGluT2-stained climbing fiber terminals (arrowheads) at both ages (***B***, ***E***). Also note that distalmost dendrites in the superficial molecular layer at P10 are labeled less strongly for DAGLα than proximal shaft dendrites (***C***). EGL, External granular layer; GL, granular layer; ML, molecular layer; PC, Purkinje cell layer. Scale bars, 10 μm.

Targeting of DAGLα to spine and excitatory synapse in developing and adult Purkinje cells

Figure 4*D* demonstrates highly localized distribution around spines in the soma, although such somatic spines were very rare at the adult stage. This observation strongly suggests that DAGLα expression is linked with the formation of spines or excitatory synapses. To test this possibility, we applied triple immunolabeling to the cerebellum at P10, when climbing fibers predominantly innervate somatic spines before translocation to dendrites (Altman, 1972; Chedotal and Sotelo, 1992). At P10, many spots of DAGLα labeling were found and discontinuously surrounded the somatic surface of almost all Purkinje cells (Fig. 7*A*,*B*). This spotty labeling was observed just beneath VGluT2-labeled large terminals [i.e., climbing fiber terminals (Fig. 7*B1*,*B2*, green)] and also beneath calbindin-labeled somatic spines (Fig. 7*B1*,*B3*, blue), indicating spine-associated or climbing fiber synapse-associated localization of DAGLα in the soma. Compared with the intense labeling on the soma and proximal dendrites, levels of DAGLα labeling were apparently low in distalmost dendrites (Fig. 7*A*), which grow actively at the border between the external granular layer and molecular layer (Yamada et al., 2000). At a

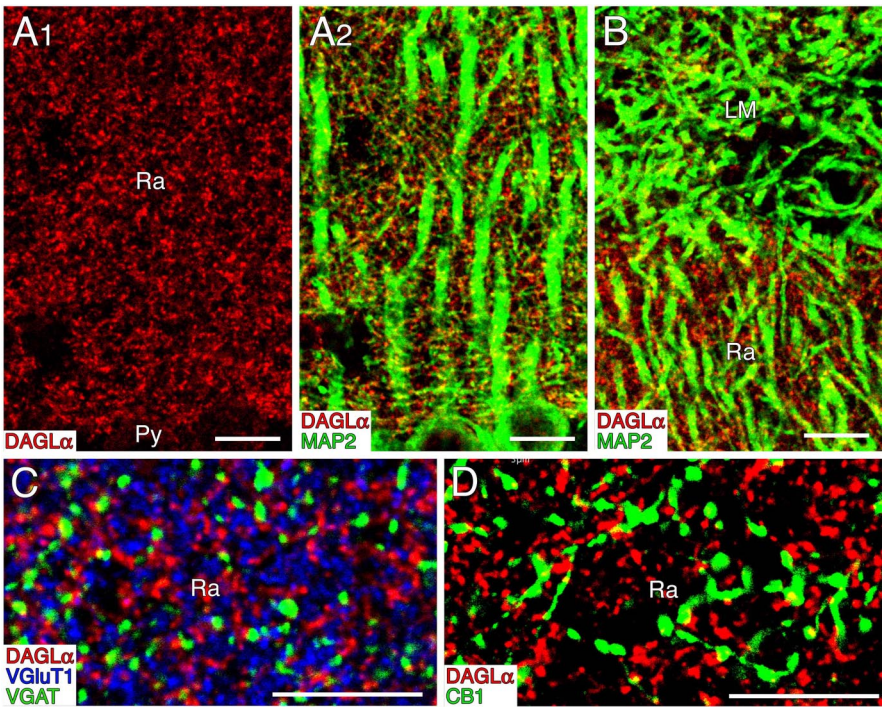

Figure 8. Immunofluorescence for DAGLα in the hippocampal CA1 region. ***A***, ***B***, Double immunostaining for DAGLα (red) and the dendritic marker MAP2 (green). Note tiny punctate labeling for DAGLα around MAP2-positive thin dendrites. ***C***, Triple immunostaining for DAGLα (red), VGAT (green), and VGluT1 (blue). ***D***, Double immunostaining for DAGLα (red) and CB1 (green). LM, Stratum lacunosum-moleculare; Py, pyramidal cell; Ra, stratum radiatum. Scale bars, 10 μm.

higher magnification, low but spotty labeling was already found on such distalmost dendrites (Fig. 7*C1*,*C2*) but was rarely associated with VGluT2-positive small terminals (Fig. 7*C3*), representing immature parallel fiber terminals (Miyazaki et al., 2003). This was also true for adult Purkinje cells (at 14 weeks of age), in which DAGLα immunolabeling on the somatic surface was localized in close association with VGluT2-labeled climbing fiber terminals (green) and calbindin-labeled somatic spines (Fig. 7*E*, blue). Together, these results support the aforementioned notion that DAGLα is targeted to particular somatodendritic sites of Purkinje cells in which spines and excitatory synapses are formed.

Spine-selective and diffuse intraspine distribution of DAGLα in hippocampal pyramidal cell

Because ERS occurs at synapses in various brain regions (Alger, 2002; Wilson and Nicoll, 2002; Piomelli, 2003), it is important to examine whether the features of DAGLα distribution found in cerebellar Purkinje cells are also applied to neurons in other brain regions. We therefore examined DAGLα distribution in hippocampal pyramidal cells, the neuron type most intensively studied so far. We found that tiny punctate labeling was predominant in the hippocampus (Fig. 8*A1*), which was apparently different from preferential somatodendritic surface labeling in the cerebellum. In the stratum radiatum of the CA1, DAGLα-labeled puncta were distributed densely around MAP2-labeled thin dendrites (Fig. 8*A2*). In contrast, DAGLα labeling was weak in intensity and few in number in the stratum lacunosum-moleculare (Fig. 8*B*). Punctate labeling for DAGLα was not overlapped with, but apposed close to, both VGluT1-labeled glutamatergic terminals and VGAT-labeled inhibitory terminals (Fig. 8*C*). Likewise, DAGLα labeling was not overlapped but often apposed closely to CB1 labeling (Fig. 8*D*). These results suggest that DAGLα is localized to certain postsynaptic structures in hippocampal pyramidal cells as well, but its fine distribution appears distinct from that in cerebellar Purkinje cells.

By immunoperoxidase (Fig. 9*A–C*) and silver-enhanced immunogold (Fig. 9*D*,*E*) electron microscopic analyses, we revealed in the CA1 stratum radiatum that DAGLα labeling was strong in dendritic spines but low or undetectable in the somatodendritic membrane. In addition, labeling pattern was variable from spine to spine. Some spines were labeled at the neck (Fig. 9*A*,*D*) or head (Fig. 9*B*,*E*) portion, whereas others were labeled at both portions (Fig. 9*C*). These patterns of immunogold labeling were quantitatively assessed in CA1 pyramidal cells. Labeling density in the cell membrane of spines was apparently higher than that of somata, shaft dendrites, and thin dendrites, and the densities in the latter elements were even higher than the background level as determined from presynaptic membrane (Fig. 9*F*). The relative tangential distribution on spine membrane was plotted from the dendrite–spine border (0%) to the edge of the postsynaptic density (100%) (Fig. 9*G*). Labeling was peaked twice, one at the base of spine neck (i.e., dendrite–spine border) and the other at the spine head.

These results suggest that DAGLα distribution is concentrated in spines of hippocampal neurons, but, within a spine, it is more widely or variably distributed compared with cerebellar Purkinje cells. However, essential features that DAGLα is closely associated with postsynaptic spines and excitatory synapses are applicable to both neuron types.

Discussion

In the present study, we have disclosed subcellular distribution of DAGLα in cerebellar Purkinje cells and hippocampal pyramidal cells. Characteristic distribution revealed in the two neurons will provide a molecular–anatomical basis for the scheme of activity-dependent synthesis of 2-AG in postsynaptic neurons and its retrograde action onto CB1-carrying presynaptic elements (Fig. 10).

Base of the spine neck is the major site of 2-AG synthesis in Purkinje cell

Distribution of DAGLα immunolabeling was highest in Purkinje cells, in which the following features were documented. First, DAGLα was detected with the C-terminal antibodies in the cytoplasmic side of the plasma membrane (Fig. 5*D*). This is consistent with the predicted molecular configuration of DAGLs that has four putative transmembrane domains with both termini inside the cell (Bisogno et al., 2003). Second, DAGLα was selective to somatodendritic elements, with the highest level in spiny branchlets and progressively decreasing toward the soma. Third, DAGLα was highly enriched at the base of spine neck but virtually excluded from the rest of the spine membrane. This particular enrichment was clearly demonstrated by the postembedding immunogold method but appreciated insufficiently by immunofluorescence and preembedding immunogold methods. The facili-

tated detection by the postembedding immunogold method suggests that molecular assembly at the base of the spine neck is tightly organized in Purkinje cells, probably for the shaping of dendritic spines and the anchoring of particular molecules, such as DAGLα.

In Purkinje cells, ERS is induced at both parallel fiber and climbing fiber synapses by either depolarization of Purkinje cells and the resultant elevation of $[Ca^{2+}]_i$ increase to ~15 μM (Kreitzer and Regehr, 2001a; Brenowitz and Regehr, 2003) or strong activation of mGluR1 (Maejima et al., 2001; Brown et al., 2003). The induction of ERS is greatly enhanced when parallel fiber stimulation is combined with climbing fiber stimulation (Brenowitz and Regehr, 2005) or when subthreshold mGluR1 activation is combined with $[Ca^{2+}]_i$ increase to a submicromolar range (Maejima et al., 2005). Parallel fibers and climbing fibers innervate spines of spiny branchlets or proximal dendrites, respectively. AMPA receptors are densely localized at the synaptic junction on the spine head and mediate fast excitatory synaptic transmission (Nusser et al., 1994), whereas mGluR1α and its downstream signaling molecules, Gαq/11 and PLCβ4, are all concentrated at the perisynaptic region on the spine head and produce DAG (Baude et al., 1993; Tanaka et al., 2000; Nakamura et al., 2004). CB1 is highly enriched at the perisynaptic region of parallel fiber terminals (Kawamura et al., 2006). Thus, the base of the spine neck is close to both the glutamate receptor-carrying postsynaptic site and the CB1-carrying presynaptic site (Fig. 10*A*). In addition, DAGLα is most densely accumulated at the base of the spine neck among DAGLα-possessing somatodendritic elements. These results suggest that the base of the spine neck is the major site of 2-AG synthesis in response to excitatory synaptic activity. This characteristic distribution would contribute to the sharpening of input specificity for endocannabinoid signaling. Our present finding that CB1 is preferentially accumulated on the synaptic side of axolemma appears important. Because the 2-AG-degrading enzyme monoglyceride lipase (MGL) is selectively localized in axons and terminals (Dinh et al., 2002; Gulyas et al., 2004), this preferential distribution would enable 2-AG to activate CB1 without passing through MGL-rich axoplasm and thereby contributes to the increasing of efficiency for endocannabinoid signaling.

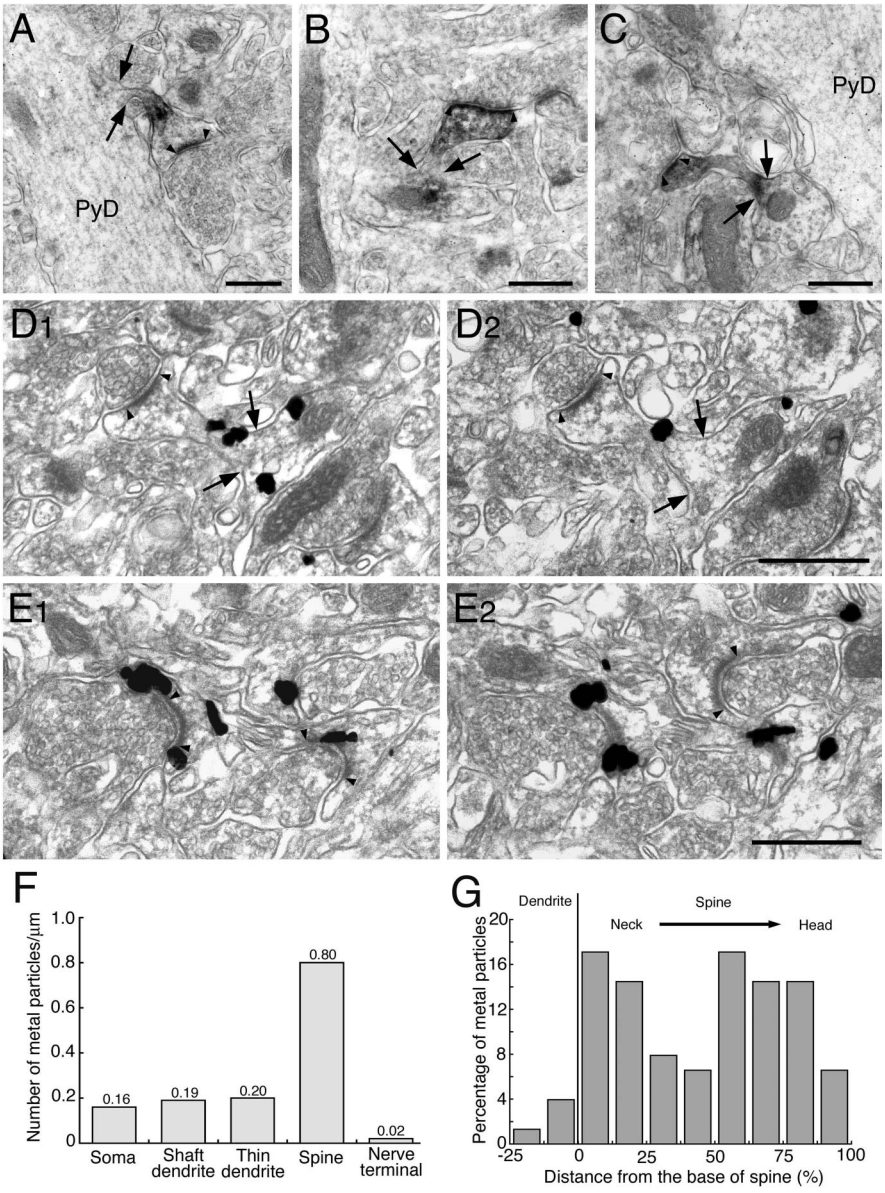

Figure 9. Immunoperoxidase (***A–C***) and silver-enhanced immunogold (***D***, ***E***) electron microscopies for DAGLα in the hippocampal CA1 region. ***A–C***, DAGLα is concentrated in dendritic spines of pyramidal cells but not in dendritic shafts (PyD). Immunoreaction products are seen in the spine neck (***A***), head (***B***), or both (***C***). ***D***, ***E***, Consecutive sections showing DAGLα labeling in the neck (***D***) and head (***E***) of spines. Arrowheads and arrows indicate the edge of postsynaptic density or the dendrite–spine border, respectively. ***F***, Histograms showing the density of preembedding immunogold labeling for DAGLα on each domain of CA1 pyramidal cells. The total length of measured cell membranes is 24.4 μm in the soma, 31.4 μm in shaft dendrites, 225.5 μm in thin dendrites, and 120.5 μm in spines. ***G***, Histograms showing the distribution of preembedding immunogold labeling in spines of CA1 pyramidal cells. The relative distance from the dendrite–spine border (0%) to the edge of the postsynaptic density (100%) is plotted in the abscissa. The ordinate indicates the percentage of metal particles in each bin, being summed from 49 spines analyzed ($n = 76$ particles). Arrows and arrowheads indicate the border between spines and dendrites (or soma) or the edge of the postsynaptic density, respectively. Scale bars, 0.5 μm.

Then why is DAGLα excluded from the spine head? DAG also functions as an activator for PKC. Like DAGLα, PKCγ is particularly abundant in Purkinje cells and activated downstream to the mGluR1 cascade (Kose et al., 1988; Nishizuka, 1992). The major mGluR1 signaling cascade in Purkinje cells, i.e., mGluR1–Gαq/11–PLCβ4–PKCγ, is crucial for climbing fiber synapse elimination and motor coordination (Kano et al., 1995, 1997, 1998; Offermanns et al., 1997). Our immunogold electron microscopy revealed wide distribution of PKCγ in Purkinje cell spines, including the head and neck portions (supplemental Fig. S1, available at www.jneurosci.org as supplemental material). One possibility is that DAGLα is excluded from the spine head so that DAG can efficiently activate PKCγ within spines, before its

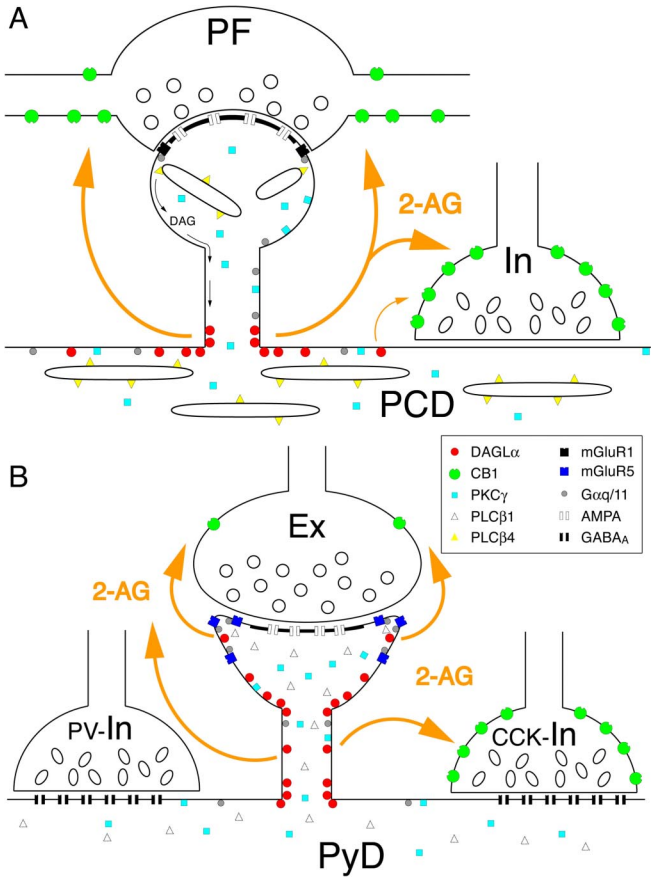

Figure 10. A scheme for endocannabinoid signaling at spiny branchlets of Purkinje cells (***A***) and hippocampal CA1 pyramidal cells (***B***), as deduced from molecular localization reported previously and in the present study. Ex, Excitatory terminal; In, inhibitory terminal; CCK-In, cholecystokinin-positive inhibitory terminal; PV-In, parvalbumin-positive inhibitory terminal; PCD, Purkinje cell dendrite; PF, parallel fiber terminal; PyD, pyramidal cell dendrite.

catalysis into 2-AG. When DAG production is increased enough to spread over to the base of the spine neck, 2-AG synthesis would be initiated and induce ERS. If DAGLα were distributed on the spine head as well, ERS would occur more preferentially and potently at the nearby excitatory synapse than at remote inhibitory synapses. Thus, the restricted localization is also likely to coordinate induction threshold and magnitude of ERS at excitatory and inhibitory synapses.

Somatodendritic surface of Purkinje cells is an additional site for 2-AG synthesis

The surface of dendritic shafts and soma is mainly innervated by inhibitory interneurons, i.e., stellate cells and basket cells. CB1 is expressed in these interneurons (Mailleux and Vanderhaeghen, 1992) and localized abundantly in their axons and terminals (Tsou et al., 1998; Kawamura et al., 2006). ERS can be induced at these inhibitory synapses after strong depolarization of Purkinje cells (Kreitzer and Regehr, 2001b; Diana et al., 2002; Yoshida et al., 2002; Brenowitz and Regehr, 2003) and by activation of group I mGluR (Galante and Diana, 2004). We show that the cell membrane of dendritic shafts and soma possess DAGLα, although at a much lower level than the base of the spine neck. The wealth of CB1 on inhibitory axons and terminals and the distribution of DAGLα on nearby somatodendritic membrane suggest that ERS is induced at inhibitory synapses by 2-AG, which is synthesized at local somatodendritic surface as well as at the base of the spine neck (Fig. 10*A*).

In adult Purkinje cells, the density of spines is much higher at spiny branchlets than at proximal dendrites, which reflects innervation territories of parallel fibers and climbing fibers (Ichikawa et al., 2002). In contrast, spines are extremely rare in the soma, because this domain is predominantly innervated by basket cell axons in adults. By pursuing occasional spotty labeling on somatic surface, we could find somatic spines and selective DAGLα labeling around the spines (Figs. 4*C*,*D*, 7*D*,*E*). At P10, when somatic spines are numerous, a number of DAGLα labeling was observed on the somatic surface just beneath climbing fiber–somatic spine synapses. Conversely, distalmost dendrites of Purkinje cells at P10 are poorly developed in terms of spinogenesis and synaptogenesis and extend filopodium-like processes instead of mature spines (Yamada et al., 2000). DAGLα was already expressed as spotty labeling on such immature dendrites (Fig. 7*C*). Therefore, DAGLα expression appears to be linked closely with the formation of spines and/or excitatory synapses, i.e., DAGLα is targeted to around spines or synapses when they are formed and matured but disappears when they are lost. This targeting mechanism will explain the distal-to-proximal gradient of DAGLα expression along the somatodendritic surface of adult Purkinje cells.

Spine is the major site of 2-AG synthesis in hippocampal pyramidal cell

CB1 and 2-AG mediates ERS in the hippocampus as well (Hajos et al., 2000; Varma et al., 2001; Wilson and Nicoll, 2001; Hashimotodani et al., 2005). We found postsynaptic expression of DAGLα in hippocampal pyramidal cells, but its subcellular distribution is different from that of Purkinje cells. DAGLα labeling was mainly present in dendritic spines. Within spines, DAGLα was detected in either the spine head or neck in some spines, whereas both portions were labeled in others. Furthermore, DAGLα labeling was dense in the stratum radiatum, whereas the labeling was considerably low in the stratum lacunosum-moleculare. This result suggests that trafficking of DAGLα is regulated in an input-selective manner in given CA1 pyramidal cells. The input-selective expression would facilitate DAGLα-mediated 2-AG synthesis at synapses receiving particular excitatory inputs, such as the Schaffer collaterals. CB1 is expressed at high levels in inhibitory terminals of cholecystokinin-positive interneurons (Katona et al., 1999; Tsou et al., 1999), whereas the level is ~20–30 times lower in excitatory terminals (Kawamura et al., 2006). Electrophysiological data demonstrate that threshold for depolarization-induced ERS is much lower at inhibitory synapses than at excitatory synapses in the hippocampus (Ohno-Shosaku et al., 2002). Although strong activation is required, ERS at hippocampal excitatory synapses might occur rather selectively at the activated synapse because of low CB1 expression in excitatory terminals and abundant expression of DAGLα, AMPA receptors (Baude et al., 1995), mGluR5 (Luján et al., 1996, 1997), Gq-protein (Tanaka et al., 2000), and PLCβ1 (our unpublished data) in postsynaptic spines (Fig. 10*B*). In contrast, ERS will be readily induced at local inhibitory synapses carrying high levels of CB1. The lack of dendritic expression of DAGLα further suggests that ERS at such inhibitory synapses is triggered by 2-AG synthesized and released from spines forming excitatory synapses.

In conclusion, DAGLα is targeted to postsynaptic spines in both cerebellar and hippocampal neurons, which should be important for efficient production of 2-AG depending on excitatory synaptic activity. The difference in its fine distribution around

spines may be attributable to differences in the synaptic organization and in the density of presynaptic CB1 between the cerebellum and hippocampus. The localization of DAGLα may be regulated so that 2-AG can readily reach presynaptic CB1 and exert its swift retrograde modulation.

References

Alger BE (2002) Retrograde signaling in the regulation of synaptic transmission: focus on endocannabinoids. Prog Neurobiol 68:247–286.

Altman J (1972) Postnatal development of the cerebellar cortex in the rat. II. Phases in the maturation of Purkinje cells and of the molecular layer. J Comp Neurol 145:399–463.

Baude A, Nusser Z, Roberts JD, Mulvihill E, McIlhinney RA, Somogyi P (1993) The metabotropic glutamate receptor (mGluR1α) is concentrated at perisynaptic membrane of neuronal subpopulations as detected by immunogold reaction. Neuron 11:771–787.

Baude A, Nusser Z, Molnar E, McIlhinney RA, Somogyi P (1995) High-resolution immunogold localization of AMPA type glutamate receptor subunits at synaptic and non-synaptic sites in rat hippocampus. Neuroscience 69:1031–1055.

Bisogno T, Howell F, Williams G, Minassi A, Cascio MG, Ligresti A, Matias I, Schiano-Moriello A, Paul P, Williams EJ, Gangadharan U, Hobbs C, Di Marzo V, Doherty P (2003) Cloning of the first sn1-DAG lipases points to the spatial and temporal regulation of endocannabinoid signaling in the brain. J Cell Biol 163:463–468.

Bodor AL, Katona I, Nyiri G, Mackie K, Ledent C, Hajos N, Freund TF (2005) Endocannabinoid signaling in rat somatosensory cortex: laminar differences and involvement of specific interneuron types. J Neurosci 25:6845–6856.

Brenowitz SD, Regehr WG (2003) Calcium dependence of retrograde inhibition by endocannabinoids at synapses onto Purkinje cells. J Neurosci 23:6373–6384.

Brenowitz SD, Regehr WG (2005) Associative short-term synaptic plasticity mediated by endocannabinoids. Neuron 45:419–431.

Brown SP, Brenowitz SD, Regehr WG (2003) Brief presynaptic bursts evoke synapse-specific retrograde inhibition mediated by endogenous cannabinoids. Nat Neurosci 6:1048–1057.

Chedotal A, Sotelo C (1992) Early development of olivocerebellar projections in the fetal rat using CGRP immunocytochemistry. Eur J Neurosci 4:1159–1179.

Devane WA, Hanus L, Breuer A, Pertwee RG, Stevenson LA, Griffin G, Gibson D, Mandelbaum A, Etinger A, Mechoulam R (1992) Isolation and structure of a brain constituent that binds to the cannabinoid receptor. Science 258:1946–1949.

Diana MA, Levenes C, Mackie K, Marty A (2002) Short-term retrograde inhibition of GABAergic synaptic currents in rat Purkinje cells is mediated by endogenous cannabinoids. J Neurosci 22:200–208.

Dinh TP, Carpenter D, Leslie FM, Freund TF, Katona I, Sensi SL, Kathuria S, Piomelli D (2002) Brain monoglyceride lipase participating in endocannabinoid inactivation. Proc Natl Acad Sci USA 99:10819–10824.

Farquhar-Smith WP, Egertova M, Bradbury EJ, McMahon SB, Rice AS, Elphick MR (2000) Cannabinoid CB1 receptor expression in rat spinal cord. Mol Cell Neurosci 15:510–521.

Freund TF (2003) Interneuron diversity series: rhythm and mood in perisomatic inhibition. Trends Neurosci 26:489–495.

Fritschy JM, Weinmann O, Wenzel A, Benke D (1998) Synapse-specific localization of NMDA and $GABA_A$ receptor subunits revealed by antigen-retrieval immunohistochemistry. J Comp Neurol 390:194–210.

Fukaya M, Watanabe M (2000) Improved immunohistochemical detection of postsynaptically located PSD-95/SAP90 protein family by protease section pretreatment: a study in the adult mouse brain. J Comp Neurol 426:572–586.

Fukudome Y, Ohno-Shosaku T, Matsui M, Omori Y, Fukaya M, Tsubokawa H, Taketo MM, Watanabe M, Manabe T, Kano M (2004) Two distinct classes of muscarinic action on hippocampal inhibitory synapses: M2-mediated direct suppression and M1/M3-mediated indirect suppression through endocannabinoid signalling. Eur J Neurosci 19:2682–2692.

Galante M, Diana MA (2004) Group I metabotropic glutamate receptors inhibit GABA release at interneuron-Purkinje cell synapses through endocannabinoid production. J Neurosci 24:4865–4874.

Gulyas AI, Cravatt BF, Bracey MH, Dinh TP, Piomelli D, Boscia F, Freund TF (2004) Segregation of two endocannabinoid-hydrolyzing enzymes into pre- and postsynaptic compartments in the rat hippocampus, cerebellum and amygdala. Eur J Neurosci 20:441–458.

Hajos N, Katona I, Naiem SS, MacKie K, Ledent C, Mody I, Freund TF (2000) Cannabinoids inhibit hippocampal GABAergic transmission and network oscillations. Eur J Neurosci 12:3239–3249.

Hajos N, Ledent C, Freund TF (2001) Novel cannabinoid-sensitive receptor mediates inhibition of glutamatergic synaptic transmission in the hippocampus. Neuroscience 106:1–4.

Hashimotodani Y, Ohno-Shosaku T, Tsubokawa H, Ogata H, Emoto K, Maejima T, Araishi K, Shin HS, Kano M (2005) Phospholipase Cβ serves as a coincidence detector through its Ca^{2+} dependency for triggering retrograde endocannabinoid signal. Neuron 45:257–268.

Howlett AC, Barth F, Bonner TI, Cabral G, Casellas P, Devane WA, Felder CC, Herkenham M, Mackie K, Martin BR, Mechoulam R, Pertwee RG (2002) International Union of Pharmacology. XXVII. Classification of cannabinoid receptors. Pharmacol Rev 54:161–202.

Ichikawa R, Miyazaki T, Kano M, Hashikawa T, Tatsumi H, Sakimura K, Mishina M, Inoue Y, Watanabe M (2002) Distal extension of climbing fiber territory and multiple innervation caused by aberrant wiring to adjacent spiny branchlets in cerebellar Purkinje cells lacking glutamate receptor δ2. J Neurosci 22:8487–8503.

Kano M, Hashimoto K, Chen C, Abeliovich A, Aiba A, Kurihara H, Watanabe M, Inoue Y, Tonegawa S (1995) Impaired synapse elimination during cerebellar development in PKCγ mutant mice. Cell 83:1223–1231.

Kano M, Hashimoto K, Kurihara H, Watanabe M, Inoue Y, Aiba A, Tonegawa S (1997) Persistent multiple climbing fiber innervation of cerebellar Purkinje cells in mice lacking mGluR1. Neuron 18:71–79.

Kano M, Hashimoto K, Watanabe M, Kurihara H, Offermanns S, Jiang H, Wu Y, Jun K, Shin HS, Inoue Y, Simon MI, Wu D (1998) Phospholipase Cβ4 is specifically involved in climbing fiber synapse elimination in the developing cerebellum. Proc Natl Acad Sci USA 95:15724–15729.

Katona I, Sperlagh B, Sik A, Kafalvi A, Vizi ES, Mackie K, Freund TF (1999) Presynaptically located CB1 cannabinoid receptors regulate GABA release from axon terminals of specific hippocampal interneurons. J Neurosci 19:4544–4558.

Katona I, Rancz EA, Acsady L, Ledent C, Mackie K, Hajos N, Freund TF (2001) Distribution of CB1 cannabinoid receptors in the amygdala and their role in the control of GABAergic transmission. J Neurosci 21:9506–9518.

Kawamura Y, Fukaya M, Maejima T, Yoshida T, Miura E, Watanabe M, Ohno-Shosaku T, Kano M (2006) The CB1 cannabinoid receptor is the major cannabinoid receptor at excitatory presynaptic site in the hippocampus and cerebellum. J Neurosci 26:2991–3001.

Kim J, Isokawa M, Ledent C, Alger BE (2002) Activation of muscarinic acetylcholine receptors enhances the release of endogenous cannabinoids in the hippocampus. J Neurosci 22:10182–10191.

Kofalvi A, Rodrigues RJ, Ledent C, Mackie K, Vizi ES, Cunha RA, Sperlagh B (2005) Involvement of cannabinoid receptors in the regulation of neurotransmitter release in the rodent striatum: a combined immunochemical and pharmacological analysis. J Neurosci 25:2874–2884.

Kose A, Saito N, Ito H, Kikkawa U, Nishizuka Y, Tanaka C (1988) Electron microscopic localization of type I protein kinase C in rat Purkinje cells. J Neurosci 8:4262–4268.

Kreitzer AC, Regehr WG (2001a) Retrograde inhibition of presynaptic calcium influx by endogenous cannabinoids at excitatory synapses onto Purkinje cells. Neuron 29:717–727.

Kreitzer AC, Regehr WG (2001b) Cerebellar depolarization-induced suppression of inhibition is mediated by endogenous cannabinoids. J Neurosci 21:RC174(1–5).

Luján R, Nusser Z, Roberts JD, Shigemoto R, Somogyi P (1996) Perisynaptic location of metabotropic glutamate receptors mGluR1 and mGluR5 on dendrites and dendritic spines in the rat hippocampus. Eur J Neurosci 8:1488–1500.

Luján R, Roberts JD, Shigemoto R, Ohishi H, Somogyi P (1997) Differential plasma membrane distribution of metabotropic glutamate receptors mGluR1α, mGluR2 and mGluR5, relative to neurotransmitter release sites. J Chem Neuroanat 13:219–241.

Maejima T, Hashimoto K, Yoshida T, Aiba A, Kano M (2001) Presynaptic inhibition caused by retrograde signal from metabotropic glutamate to cannabinoid receptors. Neuron 31:463–475.

Maejima T, Oka S, Hashimotodani Y, Ohno-Shosaku T, Aiba A, Wu D, Waku K, Sugiura T, Kano M (2005) Synaptically driven endocannabinoid re-

lease requires Ca^{2+}-assisted metabotropic glutamate receptor subtype 1 to phospholipase Cβ4 signaling cascade in the cerebellum. J Neurosci 25:6826–6835.

Mailleux P, Vanderhaeghen JJ (1992) Distribution of neuronal cannabinoid receptor in the adult rat brain: a comparative receptor binding radioautography and in situ hybridization histochemistry. Neuroscience 48:655–668.

Matsuda LA, Lolait SJ, Brownstein MJ, Young AC, Bonner TI (1990) Structure of a cannabinoid receptor and functional expression of the cloned cDNA. Nature 346:561–564.

Mechoulam R, Ben-Shabat S, Hanus L, Ligumsky M, Kaminski NE, Schatz AR, Gopher A, Almog S, Martin BR, Compton DR, Pertwee RG, Griffin G, Bayewitch M, Barg J, Vogel Z (1995) Identification of an endogenous 2-monoglyceride, present in canine gut, that binds to cannabinoid receptors. Biochem Pharmacol 50:83–90.

Melis M, Perra S, Muntoni AL, Pillolla G, Lutz B, Marsicano G, Di Marzo V, Gessa GL, Pistis M (2004) Prefrontal cortex stimulation induces 2-arachidonoyl-glycerol-mediated suppression of excitation in dopamine neurons. J Neurosci 24:10707–10715.

Miura E, Fukaya M, Sato T, Sugihara K, Asano M, Yoshioka K, Watanabe M (2006) Expression and distribution of JNK/SAPK-associated scaffold protein JSAP1 in developing and adult mouse brain. J Neurochem, in press.

Miyazaki T, Fukaya M, Shimizu H, Watanabe M (2003) Subtype switching of vesicular glutamate transporters at parallel fibre-Purkinje cell synapses in developing mouse cerebellum. Eur J Neurosci 17:2563–2572.

Nakamura M, Sato K, Fukaya M, Araishi K, Aiba A, Kano M, Watanabe M (2004) Signaling complex formation of phospholipase Cβ4 with metabotropic glutamate receptor type 1α and 1,4,5-trisphosphate receptor at the perisynapse and endoplasmic reticulum in the mouse brain. Eur J Neurosci 20:2929–2944.

Nishizuka Y (1992) Intracellular signaling by hydrolysis of phospholipids and activation of protein kinase C. Science 258:607–614.

Nusser Z, Mulvihill E, Streit P, Somogyi P (1994) Subsynaptic segregation of metabotropic and ionotropic glutamate receptors as revealed by immunogold localization. Neuroscience 61:421–427.

Offermanns S, Hashimoto K, Watanabe M, Sun W, Kurihara H, Thompson RF, Inoue Y, Kano M, Simon MI (1997) Impaired motor coordination and persistent multiple climbing fiber innervation of cerebellar Purkinje cells in mice lacking Gαq. Proc Natl Acad Sci USA 94:14089–14094.

Ohno-Shosaku T, Maejima T, Kano M (2001) Endogenous cannabinoids mediate retrograde signals from depolarized postsynaptic neurons to presynaptic terminals. Neuron 29:729–738.

Ohno-Shosaku T, Tsubokawa H, Mizushima I, Yoneda N, Zimmer A, Kano M (2002) Presynaptic cannabinoid sensitivity is a major determinant of depolarization-induced retrograde suppression at hippocampal synapses. J Neurosci 22:3864–3872.

Ohno-Shosaku T, Matsui M, Fukudome Y, Shosaku J, Tsubokawa H, Taketo MM, Manabe T, Kano M (2003) Postsynaptic M1 and M3 receptors are responsible for the muscarinic enhancement of retrograde endocannabinoid signalling in the hippocampus. Eur J Neurosci 18:109–116.

Ottersen OP, Landsend AS (1997) Organization of glutamate receptors at the synapse. Eur J Neurosci 9:2219–2224.

Piomelli D (2003) The molecular logic of endocannabinoid signalling. Nat Rev Neurosci 4:873–884.

Safo PK, Regehr WG (2005) Endocannabinoids control the induction of cerebellar LTD. Neuron 48:647–659.

Stella N, Schweitzer P, Piomelli D (1997) A second endogenous cannabinoid that modulates long-term potentiation. Nature 388:773–778.

Sugiura T, Kondo S, Sukagawa A, Nakane S, Shinoda A, Itoh K, Yamashita A, Waku K (1995) 2-Arachidonoylglycerol: a possible endogenous cannabinoid receptor ligand in brain. Biochem Biophys Res Commun 215:89–97.

Tanaka J, Nakagawa S, Kushiya E, Yamasaki M, Fukaya M, Iwanaga T, Simon MI, Sakimura K, Kano M, Watanabe M (2000) Gq protein α subunits Gαq and Gα11 are localized at postsynaptic extra-junctional membrane of cerebellar Purkinje cells and hippocampal pyramidal cells. Eur J Neurosci 12:781–792.

Tsou K, Brown S, Sanudo-Pena MC, Mackie K, Walker JM (1998) Immunohistochemical distribution of cannabinoid CB1 receptors in the rat central nervous system. Neuroscience 83:393–411.

Tsou K, Mackie K, Sanudo-Pena MC, Walker JM (1999) Cannabinoid CB1 receptors are localized primarily on cholecystokinin-containing GABAergic interneurons in the rat hippocampal formation. Neuroscience 93:969–975.

Varma N, Carlson GC, Ledent C, Alger BE (2001) Metabotropic glutamate receptors drive the endocannabinoid system in hippocampus. J Neurosci 21:RC188(1–5).

Watanabe M, Fukaya M, Sakimura K, Manabe T, Mishina M, Inoue Y (1998a) Selective scarcity of NMDA receptor channel subunits in the stratum lucidum (mossy fibre-recipient layer) of the mouse hippocampal CA3 subfield. Eur J Neurosci 10:478–487.

Watanabe M, Nakamura M, Sato K, Kano M, Simon MI, Inoue Y (1998b) Patterns of expression for the mRNA corresponding to the four isoforms of phospholipase Cβ in mouse brain. Eur J Neurosci 10:2016–2025.

Wilson RI, Nicoll RA (2001) Endogenous cannabinoids mediate retrograde signalling at hippocampal synapses. Nature 410:588–592.

Wilson RI, Nicoll RA (2002) Endocannabinoid signaling in the brain. Science 296:678–682.

Yamada K, Fukaya M, Shibata T, Kurihara H, Tanaka K, Inoue Y, Watanabe M (2000) Dynamic transformation of Bergmann glial fibers proceeds in correlation with dendritic outgrowth and synapse formation of cerebellar Purkinje cells. J Comp Neurol 418:106–120.

Yamasaki M, Yamada K, Furuya S, Mitoma J, Hirabayashi Y, Watanabe M (2001) 3-Phosphoglycerate dehydrogenase, a key enzyme for l-serine biosynthesis, is preferentially expressed in the radial glia/astrocyte lineage and olfactory ensheathing glia in the mouse brain. J Neurosci 21:7691–7704.

Yoshida T, Hashimoto K, Zimmer A, Maejima T, Araishi K, Kano M (2002) The cannabinoid CB1 receptor mediates retrograde signals for depolarization-induced suppression of inhibition in cerebellar Purkinje cells. J Neurosci 22:1690–1697.